PROCEEDINGS OF SCIENCE

QGP evolution and hadronisation

Fabio Colamaria[a,*], **for the ALICE, ATLAS, CMS and LHCb Collaborations**

[a] *Istituto Nazionale di Fisica Nucleare - Sezione di Bari,*
Via E. Orabona, 4, Bari, 70125, Italy

E-mail: fabio.colamaria@ba.infn.it, fabio.colamaria@cern.ch

Due to the extremely large temperature and energy density reached in ultra-relativistic heavy-ion collisions, a hot and dense state of matter is produced, the quark-gluon plasma (QGP), in which quarks and gluons are deconfined. Due to these properties, this short-lived state shows a very different behaviour compared to ordinary hadronic matter. In this contribution, the typical evolution of a heavy-ion collision is described, from the onset of the QGP phase to the production of final-state particles. Recent experimental results from the LHC Collaborations, allowing us to characterise the various system stages, are reported. Particular focus is given on the hadronisation stage, in which the transition from deconfined partons to hadrons occurs.

The Tenth Annual Conference on Large Hadron Collider Physics - LHCP2022
16-20 May 2022
online

*Speaker

PoS(LHCP2022)016

1. Evolution of a heavy-ion collision

The typical evolution of a ultra-relativistic heavy-ion collision taking place at hadron colliders can be divided in several subsequent stages, each characterised by specific conditions of the system produced [1]. Immediately after the collision, the system is in a non-thermalized, pre-equilibrium state, which lasts for about 1 fm/c. When thermalisation is reached, a hot and dense state of matter is produced, the quark-gluon plasma (QGP), characterised by the deconfinement of quarks and gluons, that expands following hydrodynamics laws. During the expansion, the system cools down until it reaches the temperature ($T_C \approx 156$ MeV according to lattice QCD studies [2]) at which a crossover phase transition to a hadronic gas state occurs. At this time, up to about 10 fm/c after the collision for LHC energies, confinement is restored and hadronisation of quarks into colourless hadrons takes place. When the chemical freeze-out temperature ($T_{\rm chem} \approx 156$ MeV at $\sqrt{s_{\rm NN}} = 2.76$ TeV [3]) is reached, the particle abundances of the system are frozen. Elastic interactions can still occur till the kinetic freeze-out ($T_{\rm kin} \approx 100$ MeV [1]), where the particle momentum spectra are established.

In the following, the properties of the system at each step of its evolution are described, and the most recent and relevant measurements from the LHC collaborations that allow us to retrieve information about each stage are discussed.

2. QGP phase

During its QGP phase, the system undergoes a collective motion, described by relativistic hydrodynamics. In particular, its constituents are subject to an outward boost, known as *radial flow*, which enhances their transverse momenta, $p_{\rm T}$. Additionally, if initial-state spatial anisotropies are present, they induce an anisotropy of the pressure gradients acting on the system, which causes an anisotropy of the momentum of the outgoing partons, leading to the onset of an *anisotropic flow*. Its strength can be quantified by a Fourier expansion of the final-state particle azimuthal-angle distribution $\mathrm{d}N/\mathrm{d}\varphi$.

In addition to providing crucial information on the QGP phase (see e.g. Ref. [4–6]), extensively discussed in other contributions, flow measurements and their comparison with hydrodynamic models can give access to earlier system stages. The correlation between $[p_{\rm T}]$, the event-by-event average particle momentum, and v_2, the second-order coefficient of the $\mathrm{d}N/\mathrm{d}\varphi$ Fourier expansion, is sensitive to the properties of the initial state. The ALICE Collaboration has measured a positive value of the correlation coefficient $\rho([p_{\rm T}], v_2)$ in Pb–Pb collisions at $\sqrt{s_{\rm NN}} = 5.02$ TeV and Xe–Xe collisions at $\sqrt{s_{\rm NN}} = 5.44$ TeV, in all the centrality intervals studied [7]. This result, shown in Fig. 1 (left), is qualitatively described by hydrodynamic models exploiting IP-Glasma initial conditions [8], while models using T$_{\rm R}$ENTo initial conditions [9–11] underestimate $\rho([p_{\rm T}], v_2)$ at large centralities. Similar conclusions can be derived from measurements of the ATLAS [12] and CMS [13] Collaborations. Additionally, the ATLAS Collaboration investigated the geometry of the Xe nucleus by measuring the ratio of $\rho([p_{\rm T}], v_2)$ in Xe–Xe and Pb–Pb collisions and comparing the results with predictions from T$_{\rm R}$ENTo model [14], which has large sensitivity to nuclear deformation, as shown in Fig. 1 (right). Among the different Xe nucleus deformations studied, the

data are best described by a highly-deformed triaxial nucleus geometry (with deformation parameter values $\beta = 0.2$, $\gamma = 30°$).

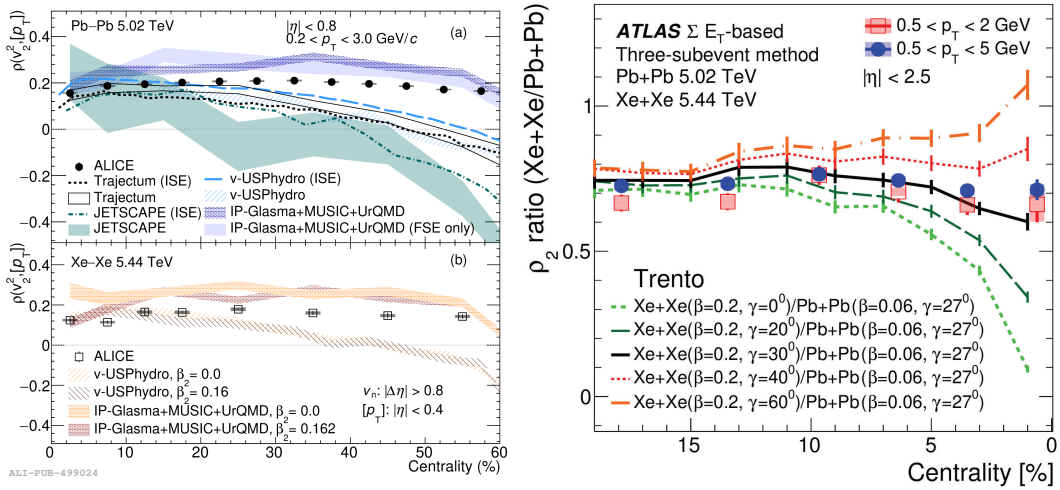

Figure 1: Left: correlation coefficient $\rho([p_T], v_2)$, measured by the ALICE Collaboration in Pb–Pb and Xe–Xe collisions as a function of centrality [7] and compared with model predictions using IP-Glasma [8] or T_RENTo initial conditions (Trajectum [9], JETSCAPE [10], v-USPhydro [11]). Right: ratio of $\rho([p_T], v_2)$ in Pb–Pb and Xe–Xe collisions measured by the ATLAS Collaboration [12], compared with T_RENTo predictions for different Xe nucleus deformations [14].

3. Hadronisation

At the phase transition to hadronic matter, the colour-charge confinement mechanism forces quarks and gluons to bind into hadrons, as in ordinary matter. Hadron abundances can be derived from the thermal composition of a hadron-resonance gas in thermal equilibrium. In this regards, statistical hadronisation models [15–18] are able to predict the p_T-integrated production yields of a large set of particle species in central heavy-ion collisions, with only three parameters obtained by fitting data: the chemical freeze-out temperature T_{chem}, the system volume V, and the baryochemical potential μ_B. A fit to the large set of particle abundances measured by the ALICE Collaboration (Ref. [19] for Pb–Pb collisions at $\sqrt{s_{NN}} = 2.76$ TeV, preliminary results available for Pb–Pb collisions at $\sqrt{s_{NN}} = 5.02$ TeV) allowed for estimating the chemical freeze-out temperature. The resulting value of T_{chem} (153 ± 2 MeV for GSI-Heidelberg model [16, 17], compatible values for the other available models) is very close to the phase transition temperature T_c.

A recent extension of the statistical hadronisation model to charm hadrons (SHMc) has been proposed by the GSI-Heidelberg group [20]. Given their large mass, charm-quark thermal production in the QGP is strongly suppressed even at LHC energies and significantly smaller than the initial production via hard-scattering processes. The fact that charm quarks are not in chemical equilibrium with the medium is accounted for by introducing fugacity factors that increase the predicted charm-hadron yields and that depend on the measured $c\bar{c}$ production cross section. Figure 2 shows the predicted p_T-integrated yields of the main charm-hadron species at midrapidity in 0–10%

central Pb–Pb collisions at $\sqrt{s_{\rm NN}}$ = 5.02 TeV, compared to measurements from the ALICE Collaboration [21–25]. The SHMc predictions successfully describe the data within the uncertainties, including the yield of Λ_c^+ baryon, if an augmented set of excited charm-baryon states is considered, not yet observed but postulated by the Relativistic Quark Model [26]. This agreement supports the hypothesis of charm-quark thermalisation in the QGP.

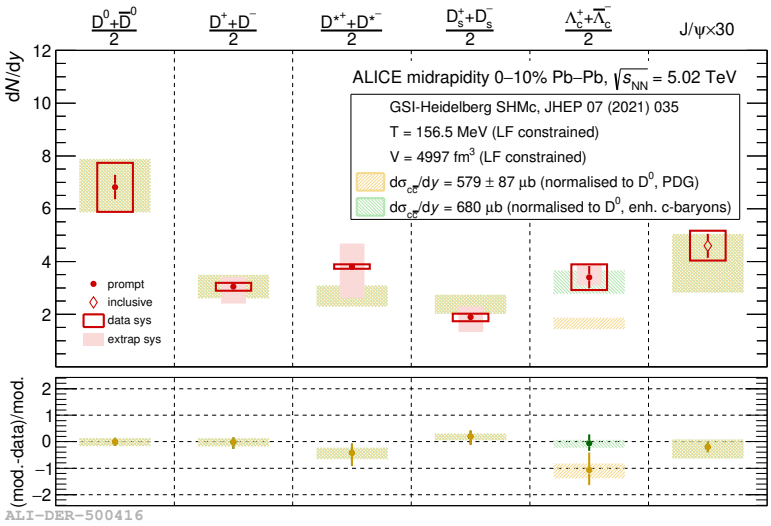

Figure 2: ALICE measurements of $p_{\rm T}$-integrated charm-hadron yields in 0–10% central Pb–Pb collisions at $\sqrt{s_{\rm NN}}$ = 5.02 TeV [21–25], compared to predictions from SHMc [20].

The large quark-density environment characterising the QGP can alter the formation mechanism of hadrons, compared to in-vacuum hadronisation, which occurs via parton fragmentation. When the QGP hadronises, quarks close in phase space can *coalesce* into colourless hadrons. This coalescence mechanism, dominant in the low and intermediate $p_{\rm T}$ range, is expected to modify the final-state hadron spectra measured in heavy-ion collision with respect to proton–proton (pp) measurements. One typical feature is the enhancement of baryon-to-meson production yields at intermediate $p_{\rm T}$ ($\approx$ 2–6 GeV/c), observed e.g. for $\Lambda/{\rm K}^0_{\rm s}$ by the ALICE Collaboration in Pb–Pb central collisions at $\sqrt{s_{\rm NN}}$ = 5.02 TeV [27].

A very similar feature has been recently observed by ALICE in the charm sector. Figure 3 shows the$p_{\rm T}$-differential $\Lambda_c^+/{\rm D}^0$ yield ratios measured at midrapidity in Pb–Pb collisions, for two different centrality ranges [23]. A 3.7σ enhancement of the Λ_c^+ production in 0–10% central Pb–Pb collisions compared to pp collisions is observed for the $4 < p_{\rm T} < 8$ GeV/c interval. It can be explained with an interplay of radial flow, which provides a larger $p_{\rm T}$ boost to heavier particles, and coalescence mechanism, which produces baryons at higher $p_{\rm T}$ than mesons. Models including these features are able to qualitatively describe the measurements.

The ALICE Collaboration has also measured the $p_{\rm T}$-differential nuclear modification factor ($R_{\rm AA}$) of prompt and non-prompt ${\rm D}_{\rm s}^+$ mesons at midrapidity, in Pb–Pb collisions at $\sqrt{s_{\rm NN}}$ = 5.02 TeV [28]. The results are shown in Fig. 4 (left), compared to equivalent measurements of non-prompt ${\rm D}^0$ mesons and predictions from the TAMU transport model [29]. A hint of a larger $R_{\rm AA}$ of non-prompt ${\rm D}_{\rm s}^+$ compared to prompt ${\rm D}_{\rm s}^+$ in the $4 < p_{\rm T} < 12$ GeV/c interval is observed. Such feature is induced by the dead-cone effect, which suppresses the forward gluon radiation inside an angular

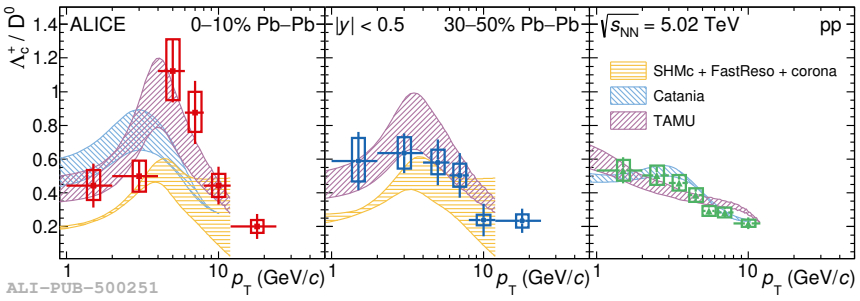

Figure 3: ALICE measurements of Λ_c^+/D^0 production yield ratios at midrapidity in 0–10% central Pb–Pb collisions (left), 30–50% central Pb–Pb collisions (middle), and pp collisions (right), at $\sqrt{s_{NN}} = 5.02$ TeV [23]. The measurements are compared with models including coalescence contribution to hadron formation.

region larger for heavier quarks, leading thus to a lower energy loss for beauty quarks. A hint for a reduced suppression of the non-prompt D_s^+ with respect to non-prompt D^0 is observed for $p_T < 6$ GeV/c, in 0–10% central collisions. This effect can be ascribed to an increased production of beauty-strange mesons from the coalescence mechanism in a strangeness-rich environment as the QGP. The TAMU model [30], which allows the formation of hadrons via coalescence, qualitatively describes the p_T trend of the results, though it tends to overestimate non-prompt D_s^+ R_{AA} measurement for $p_T > 6$ GeV/c.

Further insight on this topic was obtained by the CMS Collaboration, which performed a direct reconstruction of different beauty-meson species in Pb–Pb collisions at $\sqrt{s_{NN}} = 5.02$ TeV [31]. Figure 4 (right) shows the nuclear modification factor of B^+, B_s^0, and B_c^+ mesons at midrapidity compared to the R_{AA} of other particle species. While at high p_T the R_{AA} for all hadron species converge toward similar values, below $\approx$ 15 GeV/c there is a hint of a larger R_{AA} for B_s^0 and B_c^+ mesons, compared to the other particles. Such trend could be expected in the presence of a relevant contribution of quark coalescence for the formation of beauty-charm and beauty-strange mesons.

4. Hadronic phase

During the hadron-gas phase, between chemical and kinetic freeze-out, the system is composed of hadrons undergoing only elastic interactions, and the particle abundances are mostly fixed. Hadronic resonances constitute an important tool for studying this stage. As for the other hadron species, their production yields at the chemical freeze-out are expected to follow thermal weights, but interaction processes occurring during the hadron-gas phase can modify their yields. In particular, elastic scatterings among the resonance decay particles (rescattering) can modify their kinematics, preventing the resonance reconstruction; conversely, new resonances can be formed by the scatterings of hadrons (regeneration). The relative balance of these effects depends on the hadronic phase duration (typically of $\approx 5-10$ fm/c at LHC energies) and on the lifetimes of the resonances. Measurements of the resonance yields, compared to the yields of their stable counterparts, can thus probe the duration and properties of the hadronic phase.

The ALICE Collaboration has released preliminary measurements of the $\Lambda(1520)/\Lambda$ yield ratio for different event multiplicities, increasing from pp to Pb–Pb collisions, as shown in Fig. 5 (left).

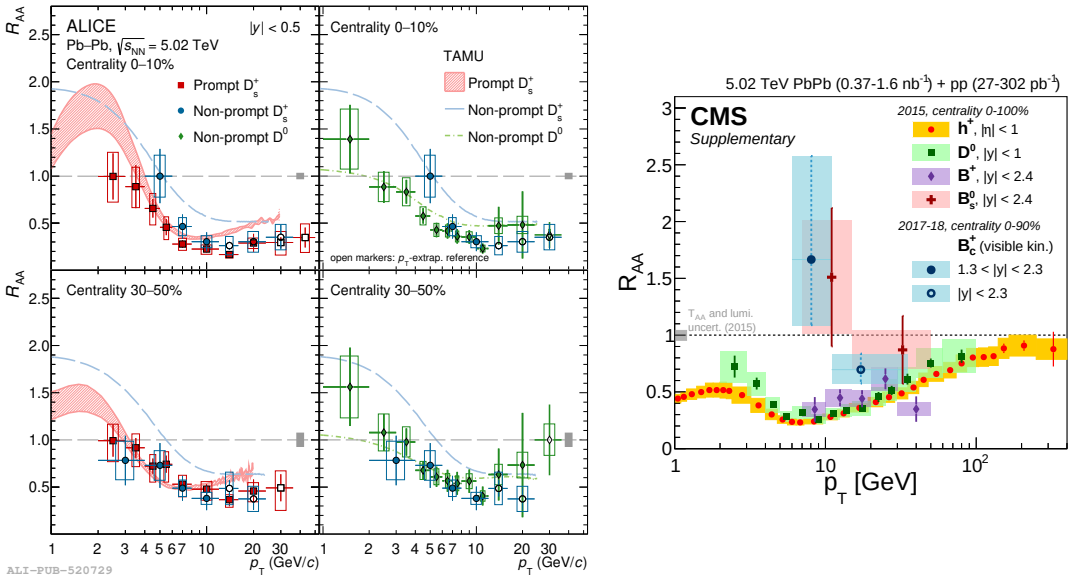

Figure 4: Left: ALICE measurements of prompt D_s^+, non-prompt D_s^+, and non-prompt D^0 nuclear modification factor in Pb–Pb collisions at $\sqrt{s_{NN}}$ = 5.02 TeV [28]. Right: nuclear modification factor of B_c^+, B_s^0 and B^+ mesons measured by CMS in Pb–Pb collisions at $\sqrt{s_{NN}}$ = 5.02 TeV [31].

While no multiplicity dependence is observed in pp collisions, the ratio progressively reduces for increasing multiplicity values in Pb–Pb, corresponding to a larger system size. A suppression of the ratio with significance 7.1σ is observed between central and most peripheral for Pb–Pb collisions. Such feature provides a clear indication for the existence of a hadronic phase, in which for the $\Lambda(1520)$ the rescattering mechanism dominates over the regeneration mechanism. A comparison with different model predictions is also presented. Statistical hadronisation models overpredict the ratio yields in central Pb–Pb collisions, where such models can be applied. As shown for the case of MUSIC [32], hydrodynamic models are instead able to reproduce the multiplicity dependence of the measurements when they are coupled with a hadronic-phase afterburner (SMASH [33]), which handles the interaction processes involving resonance formation and dissociation.

Recently, an innovative application of femtoscopic techniques has been developed to probe the strength of the residual strong interaction acting in systems of hadrons close in space. By measuring the two-particle correlation function as a function of their relative momentum, and assuming a specific spatial extension and shape for the source of the particle production, the wave function of the two-particle system can be calculated, using the Koonin-Pratt equation [34]. In this way, access to the interaction potential between the two particles is obtained. The ALICE Collaboration has investigated the charm-light hadron residual strong interaction in high-multiplicity pp collisions. Preliminary results for the final-state strong interaction for the Dπ system indicate a feeble final-state strong interaction acting between the two particles. In Fig. 5 (right), the measurement of the scattering lengths for the two isospin states $I = 3/2$ and $I = 1/2$ is shown. Calculations from lattice QCD correctly describe the scattering length for the $I = 3/2$ state, but significantly overestimate its value for the $I = 1/2$ state. Transposed to heavy-ion collisions, these results shed light about the strength of hadron interaction during the hadron-gas phase, and point toward a small probability of

rescattering for D mesons during this stage.

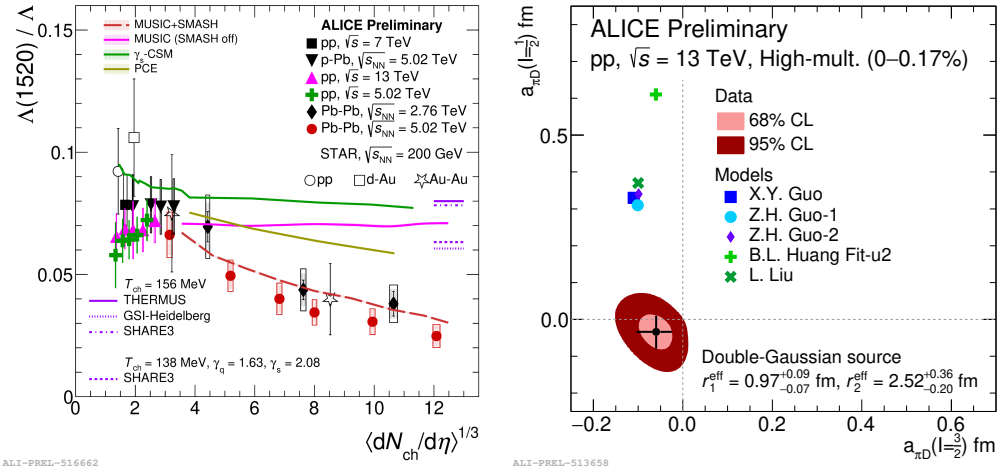

Figure 5: Left: ALICE measurements of $\Lambda(1520)/\Lambda$ yield ratios as a function of event multiplicity in pp, p–Pb, and Pb–Pb collisions, compared to expectations from statistical hadronisation models and hydrodynamic models. Right: scattering lengths for the Dπ system measured by the ALICE Collaboration in high-multiplicity pp collisions at $\sqrt{s}$ = 13 TeV.

5. Kinetic freeze-out

At the time of the kinetic freeze-out, the elastic interactions between the particles cease, and their p_{T} spectra are not modified anymore. The system is now composed of a free stream of particles, that travel towards the experimental apparatus for detection. The kinematics of the system at T_{kin} can be probed by measuring the p_{T} distribution of identified hadron species. In particular, for Pb–Pb collisions, a multiplicity-dependent hardening of these distribution is observed, which can be interpreted as the effect of the momentum boost provided by the hydrodynamical radial expansion of the system. This effect can be parameterised by means of the Boltzmann-Gibbs Blast-Wave model [35], which considers the system as a thermalised medium in radial expansion with a common velocity field, undergoing an instantaneous kinetic freeze-out at T_{kin}.

By simultaneously fitting the p_{T} spectra of different hadron species at various centralities with the Blast-Wave model, the average radial velocity β_{T} of the system and the kinetic freeze-out temperature T_{kin} can be extracted. From the measurement performed by the ALICE Collaboration in Pb–Pb collisions at $\sqrt{s_{\mathrm{NN}}}$ = 5.02 TeV [36], it can be observed that more central events reach kinetic freeze-out later (lower T_{kin}) and show a larger average radial-flow velocity ($\beta_{\mathrm{T}} = 0.663 \pm 0.003$ for the most central collisions).

In conclusion, a complete and detailed description of the QGP evolution has been obtained from the measurements performed at the LHC exploiting the data collected during Run1 and Run2. Following the LHC restart after the Long Shutdown 2, thanks to the larger data samples expected and to the improved performance of several detectors, further and more precise results are expected, which will shed further details on the specific system evolution stages.

References

[1] W. Busza, K. Rajagopal and W. van der Schee, *Heavy Ion Collisions: The Big Picture, and the Big Questions*, *Ann. Rev. Nucl. Part. Sci.* **68** (2018) 339 [1802.04801].

[2] J.N. Guenther, *Overview of the QCD phase diagram: Recent progress from the lattice*, *Eur. Phys. J. A* **57** (2021) 136 [2010.15503].

[3] A. Andronic, P. Braun-Munzinger, K. Redlich and J. Stachel, *Decoding the phase structure of QCD via particle production at high energy*, *Nature* **561** (2018) 321 [1710.09425].

[4] ALICE collaboration, *Higher harmonic flow coefficients of identified hadrons in Pb-Pb collisions at* $\sqrt{s_{\rm NN}} = 2.76$ *TeV*, *JHEP* **09** (2016) 164 [1606.06057].

[5] ALICE collaboration, *Anisotropic flow of identified particles in Pb-Pb collisions at* $\sqrt{s_{\rm NN}} = 5.02$ *TeV*, *JHEP* **09** (2018) 006 [1805.04390].

[6] ALICE collaboration, *Anisotropic flow and flow fluctuations of identified hadrons in Pb−Pb collisions at* $\sqrt{s_{\rm NN}} = 5.02$ *TeV*, 2206.04587.

[7] ALICE collaboration, *Characterizing the initial conditions of heavy-ion collisions at the LHC with mean transverse momentum and anisotropic flow correlations*, 2111.06106 CERN-EP-2021-232, [2111.06106].

[8] B. Schenke, C. Shen and D. Teaney, *Transverse momentum fluctuations and their correlation with elliptic flow in nuclear collision*, *Phys. Rev. C* **102** (2020) 034905 [2004.00690].

[9] G. Nijs, W. van der Schee, U. Gürsoy and R. Snellings, *Transverse Momentum Differential Global Analysis of Heavy-Ion Collisions*, *Phys. Rev. Lett.* **126** (2021) 202301 [2010.15130].

[10] JETSCAPE collaboration, *Phenomenological constraints on the transport properties of QCD matter with data-driven model averaging*, *Phys. Rev. Lett.* **126** (2021) 242301 [2010.03928].

[11] G. Giacalone, F.G. Gardim, J. Noronha-Hostler and J.-Y. Ollitrault, *Correlation between mean transverse momentum and anisotropic flow in heavy-ion collisions*, *Phys. Rev. C* **103** (2021) 024909 [2004.01765].

[12] ATLAS collaboration, *Correlations between flow and transverse momentum in Xe+Xe and Pb+Pb collisions at the LHC with the ATLAS detector: a probe of the heavy-ion initial state and nuclear deformation*, CERN-EP-2022-052.

[13] CMS collaboration, *Correlations between multiparticle cumulants and mean transverse momentum in small collision systems with the CMS detector*, CMS-PAS-HIN-21-012.

[14] B. Bally, M. Bender, G. Giacalone and V. Somà, *Evidence of the triaxial structure of* ^{129}*Xe at the Large Hadron Collider*, *Phys. Rev. Lett.* **128** (2022) 082301 [2108.09578].

[15] S. Wheaton, J. Cleymans and M. Hauer, *Thermus – a thermal model package for root*, *Computer Physics Communications* **180** (2009) 84.

[16] A. Andronic, P. Braun-Munzinger and J. Stachel, *Thermal hadron production in relativistic nuclear collisions: The hadron mass spectrum, the horn, and the qcd phase transition*, *Physics Letters B* **673** (2009) 142.

[17] A. Andronic, P. Braun-Munzinger, J. Stachel and H. Stöcker, *Production of light nuclei, hypernuclei and their antiparticles in relativistic nuclear collisions*, *Physics Letters B* **697** (2011) 203.

[18] M. Petran, J. Letessier, J. Rafelski and G. Torrieri, *Share with charm*, *Computer Physics Communications* **185** (2014) 2056.

[19] ALICE collaboration, *Production of ^{4}He and $^4\overline{\text{He}}$ in Pb-Pb collisions at $\sqrt{s_{\rm NN}} = 2.76$ TeV at the LHC*, *Nucl. Phys. A* **971** (2018) 1 [1710.07531].

[20] A. Andronic, P. Braun-Munzinger, M.K. Köhler, A. Mazeliauskas, K. Redlich, J. Stachel et al., *The multiple-charm hierarchy in the statistical hadronization model*, *JHEP* **07** (2021) 035 [2104.12754].

[21] ALICE collaboration, *Prompt D^0, D^+, and D^{*+} production in Pb–Pb collisions at $\sqrt{s_{\rm NN}} = 5.02$ TeV*, *JHEP* **01** (2022) 174 [2110.09420].

[22] ALICE collaboration, *Measurement of prompt D_s^+-meson production and azimuthal anisotropy in Pb–Pb collisions at $\sqrt{s_{NN}}$=5.02TeV*, *Phys. Lett. B* **827** (2022) 136986 [2110.10006].

[23] ALICE collaboration, *Constraining hadronization mechanisms with Λ_c^+/D^0 production ratios in Pb-Pb collisions at $\sqrt{s_{\rm NN}}$ = 5.02 TeV*, 2112.08156.

[24] ALICE collaboration, *Centrality and transverse momentum dependence of inclusive J/ψ production at midrapidity in Pb–Pb collisions at sNN=5.02 TeV*, *Phys. Lett. B* **805** (2020) 135434 [1910.14404].

[25] ALICE collaboration, *Inclusive J/ψ production at mid-rapidity in pp collisions at $\sqrt{s} = 5.02$ TeV*, *JHEP* **10** (2019) 084 [1905.07211].

[26] D. Ebert, R.N. Faustov and V.O. Galkin, *Spectroscopy and Regge trajectories of heavy baryons in the relativistic quark-diquark picture*, *Phys. Rev. D* **84** (2011) 014025 [1105.0583].

[27] ALICE collaboration, *K_S^0 and Λ Production in Pb–Pb Collisions at $\sqrt{s_{NN}}$ = 2.76 TeV*, *Phys. Rev. Lett.* **111** (2013) 222301.

[28] ALICE collaboration, *Measurement of beauty-strange meson production in Pb−Pb collisions at $\sqrt{s_{\rm NN}}$ = 5.02 TeV via non-prompt $\rm D_s^+$ mesons*, 2204.10386 CERN-EP-2022-065, [2204.10386].

[29] M. He and R. Rapp, *Hadronization and Charm-Hadron Ratios in Heavy-Ion Collisions*, *Phys. Rev. Lett.* **124** (2020) 042301 [1905.09216].

[30] M. He, R.J. Fries and R. Rapp, *Heavy Flavor at the Large Hadron Collider in a Strong Coupling Approach*, *Phys. Lett. B* **735** (2014) 445 [1401.3817].

[31] CMS collaboration, *Observation of the B_c^+ Meson in Pb-Pb and pp Collisions at $\sqrt{s_{NN}}$=5.02 TeV and Measurement of its Nuclear Modification Factor*, *Phys. Rev. Lett.* **128** (2022) 252301 [2201.02659].

[32] B. Schenke, S. Jeon and C. Gale, *(3+1)D hydrodynamic simulation of relativistic heavy-ion collisions*, *Phys. Rev. C* **82** (2010) 014903 [1004.1408].

[33] J. Weil et al., *Particle production and equilibrium properties within a new hadron transport approach for heavy-ion collisions*, *Phys. Rev. C* **94** (2016) 054905 [1606.06642].

[34] ALICE collaboration, *Unveiling the strong interaction among hadrons at the LHC*, *Nature* **588** (2020) 232 [2005.11495].

[35] E. Schnedermann, J. Sollfrank and U.W. Heinz, *Thermal phenomenology of hadrons from 200-A/GeV S+S collisions*, *Phys. Rev. C* **48** (1993) 2462 [nucl-th/9307020].

[36] ALICE collaboration, *Production of charged pions, kaons, and (anti-)protons in Pb-Pb and inelastic pp collisions at $\sqrt{s_{NN}} = 5.02$ TeV*, *Phys. Rev. C* **101** (2020) 044907 [1910.07678].